Residual

A **residual** is generally a quantity left over at the end of a process

Geol: that remaining after soluble elements have been dissolved and removed

something that remains to discomfort or disable a person following an operation

Latin: *residu(um) -uus* deverbal adj. suffix + **-al**

354. Fellenius, B.H., 2015. Static tests on instrumented piles affected by residual load. Journal of the Deep Foundation Institute, 9(1) 11-20.

Technical Note, Journal of the Deep Foundation Institute, 9(1) 11-20

STATIC TESTS ON INSTRUMENTED PILES AFFECTED BY RESIDUAL LOAD

Bengt H. Fellenius. Dr.Tech., P.Eng.

ABSTRACT Analysis of results from a static loading tests on an instrumented pile usually assumes that the strain-gage determined loads represent the true loads in the test pile. However, more often than not, residual load will have been present in the pile at the start of the static test. Disregarding these in the analysis will misrepresent the load-movement response and the loads determined from the strain-gage instrumentation, as presented in the paper. The results of three static loading tests: a 400-mm diameter, 45 m long, concrete-filled, closed-toe, steel-pipe pile driven in soft clay, a 460-mm diameter, 22 m long bored pile (screw-pile) in silt and sand and stiff clay, and a 600-mm diameter, 15 m long, jacked-in concrete pile in a residual, dense, silty sandy weathered sandstone. The measured load distributions are corrected for residual load, demonstrating the interdependence of the distributions of "False" and "True" distributions of load.

KEYWORDS static loading tests, residual load, instrumented piles, load distribution, full-scale test, driven precast concrete pile, driven steel pipe pile, jacked-in cylinder pile.

INTRODUCTION

A static loading test in its simplest form consists of adding increments of load to the pile head while monitoring the resulting pile head movement. Instrumenting the pile will enhance the information provided by the test. Instrumentation usually consists of strain-gages placed at selected depths in the pile to serve for determining the distribution of axial load in the pile during the test. The conversion from measured strain to load is relatively straight-forward. However, the common belief that the so-determined load is the load actuallypresent in the pile is often mistaken.

Before the test, piles are frequently subject to locked-in loads, called "residual load", as early on was demonstrated by Nordlund (1963), Hunter and Davison (1969), and Gregersen et al. (1973). The following three case histories contain results from static loading tests where the strain-gage results were clearly affected by residual load. One case involves a pipe pile driven into soft clay, one a bored pile constructed through silt, sand, and stiff clay, and the third a spun-pile installed into a firm to stiff clay by jack-in procedure.

Consulting Engineer
2475 Rothesay Avenue, Sidney, BC, Canada, V8L 2B9
E: bengt@fellenius.net

RESIDUAL LOAD

Residual load (also called residual force or locked-in force) in a pile is the axial force present in a pile at the outset of a static loading test. It develops during the last impact given to a driven pile and, for both driven and bored piles, during the "recovery" of the soil after the disturbance from the construction. For the driven pile, the upward movement of the pile toe in unloading from the last impact is incomplete because of the spring action being resisted by the shaft resistance, resulting in a residual toe load and a residual counteracting load distributed along the pile shaft. Subsequent to the construction, small settlements of the surrounding soil may develop, which adds load to the residual load already present in the pile. This load is resisted over the lower pile length where positive shaft resistance will develop. A force equilibrium will appear (much is the same way as a pile is subjected to drag force and a neutral plane development under long-term conditions). The soil movements may be small, but are often large enough to mobilize fully the shaft resistance at least in the upper and lower lengths of the pile with a transition zone along an in-between length, embracing the boundary between shaft resistance in negative direction above and positive direction below the neutral plane.

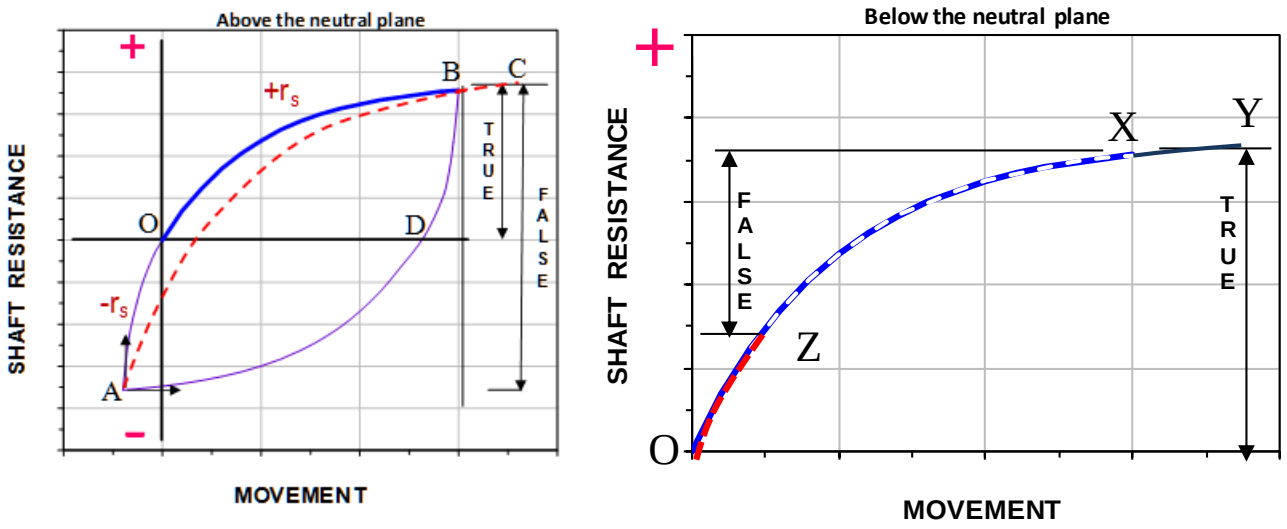

Fig. 1 Hysteresis loops for the shaft resistance mobilized in a static loading test for the case of no residual load and for presence of residual load above and below the neutral plane

The loads applied to the pile head in a test on a pile that has developed residual load will first reduce the negative skin friction along the upper length and, then, mobilize additional positive shaft resistance along loads. However, the difference between the two the lower length. The mechanism along the pile shaft is a similar to the shaft hysteresis loops illustrated in Figure 1 showing the mobilized shaft shear versus the movement between the pile and the soil above and below the neutral plane. If no residual load is present in the pile at the start of the test, the starting point is the origin, O, and the shaft shear is mobilized along Path O-B and on to C. Point B is here assumed to represent approximately fully mobilized shaft resistance.

Above the neutral plane, residual load develops as negative skin friction along Path D-A (After unloading via Path B-D with Point D the origin of the residual load development). In a subsequent static loading test, the shaft shear is mobilized along Path A-O-B. The residual load is first unloaded—reduced—along Path A-O. The continued development then builds up shaft resistance along Path O-B. However, if the presence of residual load is not recognized, the response will be thought as representing Path O-B, only, because it is not realized that negative skin friction has first to be overcome along Path A-O. Thus the belief of residual load not being present in the pile will indicate a "false" resistance that is twice as large as the "true" resistance (assuming that also Point A represents ultimate shaft resistance condition—i.e., fully mobilized negative skin friction). The movement along Path A-O-B, will be only slightly larger than the virgin movement along Path O-B, would have been.

Below the neutral plane, the effect of the residual load is more straight-forward. The residual load develops as positive shaft resistance along Path O-Z and in the test the fully mobilized shaft resistance at Point X is reached along Path Z-B. If the presence of residual load is not recognized, Path Z-B will be thought as representing Path O-B and the ultimate shaft resistance will be underestimated, as will the movement necessary to mobilize it. In the extreme, if the residual load is built up of fully mobilized positive shaft resistance, then, the impression will be that there is no resistance along that length of the pile.

The pile toe response is illustrated in Figure 2. Similar to the shaft resistance development, when no residual load is present, the mobilization of the toe resistance is along Path O-X-Y. However, if residual toe load is present, then, the response is along Path Z-X-Y. If the presence of residual load is unrecognized, it will be believed that the response started from zero, i.e., Point Z will be believed to be the origin, Point O, and the toe load will be underestimated.

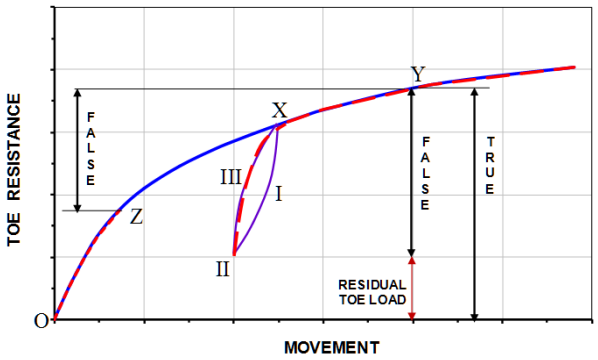

Fig. 2 The toe resistance response mobilized in a static loading test for the case of no residual load and for presence of residual load

For a driven or a jacked-in pile, or if the pile construction has involved a prior cycle of loading, the residual load is the load remaining from an unloading of the pile toe from Point X along Path X-I-II. In the loading test, the toe response will then be along Path II-III-X-Y. Now, the toe load is not only underestimated, the shape of the toe load-movement response will show a break in the reloading curve at Point B that can easily be mistaken for a failure load and be so stated. In fact, it is a rather common mistake.

STEEL PIPE PILE IN SANDPOINT, IDAHO

A full-scale head-down test was performed 48 days after driving an instrumented, 406-mm diameter, 45 m long, concrete-filled, closed-toe, steel pipe pile in Sandpoint, Idaho, into a deposit of glacial clay (Fellenius et al. 2004). The purpose of the test was to establish the shaft resistance distribution and, thus, the pile embedment length necessary to support loads from a bridge abutment.

The soil profile consists of 9 m of sand followed by 41 m of soft clay (with sand lenses) on 3 m of compact sand, 10 m of firm silty clay, 6 m of compact to dense sand, and, then, soft to firm clay and silt to depths exceeding 200 m. The groundwater table lies at 4.5 m depth and the pore pressure distribution is hydrostatic. Figure 3 presents the results of a CPTU sounding performed at the test pile location. The friction ratio in the clay layers (depths 9 through 50 m and below 66 m) ranges from 0.2 % to 0.3 %, which is smaller than usually found for clays. Such a small range is indicative for sensitive clay. Driving piles in sensitive clay more or less completely remolds the clay along the pile shaft. The subsequent reconsolidation and settlement cause the clay to hang on the pile, which results in considerable residual load.

The pile was instrumented with diametrically opposed pairs of vibrating-wire strain-gages at eight depths in the pile: 1.3, 6.5, 10.1, 16.9, 23.9, 30.9, 38.0, and 44.9 m. The static loading test was performed by adding equal increments of 150 kN at 10-minute intervals until the pile failed in plunging when the applied load was 1,910 kN. Figure 4 shows the load-movement curves from the static loading test, which indicate that the plunging failure occurred at a pile head movement of about 10 mm and a toe movement of about 3 mm. For reference, the figure also includes the Offset Limit line, which intersection with the pile-head load-movement curve is a conservative definition of pile capacity determined from a static loading test (Davison 1972, Fellenius 2015).

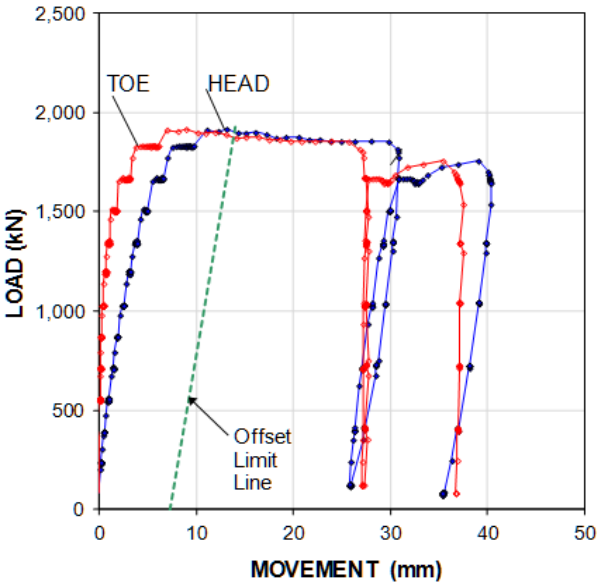

Fig. 4 Load-movement curves for pile head and pile toe. Load vs. pile head movement, Case 1

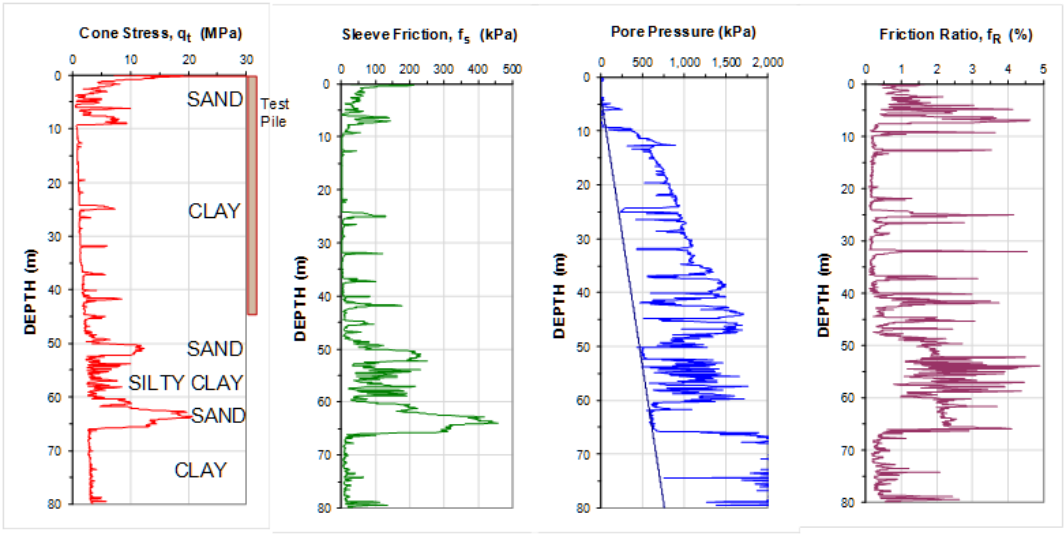

Fig. 3 Results of CPTU sounding next to the test pile location, Case 1

Figure 5 shows the load distribution evaluated from the eight strain-gage levels. The apparent tension in the pile after unloading is due to a release of the residual load in the pile (the pile actually rebounded to longer total length than its length before the test). The most remarkable result shown by the load distribution is that no shaft resistance seems to have been mobilized along the lower 15 m length of the pile. This is due to the fact that, below about 30 m depth, the residual load is built up of fully mobilized, positive shear resistance.

The distribution obtained from the strain-gage determined loads is the "False" distribution. Fellenius (2002a; 2002b) developed a direct method for correcting the "False" resistance distribution for the residual load, to obtain the "True" distribution. The method builds on the assumption that negative skin friction in the upper length of the pile is fully mobilized before the start of the test. The load applied to the pile head in the test must first overcome the negative direction shear forces and, then, mobilize the positive direction forces, as demonstrated in Figure 1. As the value of the ultimate shear resistance is independent of the direction of movement, the "False Resistance" distribution in the upper length of the pile then reflects the shaft resistance twice, so to speak. Thus, half the "False " distribution is the negative direction shear force (Path A-O in Figure 1) and the other half is the positive shear force (Path O-B in Figure 1).

The "True" distribution can be obtained by plotting a distribution curve exactly half way between the vertical from the applied load and the measured distribution as indicated in Figure 6. Half that distance is also the "Residual Load" distribution as plotted separately in the figure. Below some depth, the negative skin friction building up the residual load starts to reduce from being fully mobilized negative skin friction and gradually changing over to fully mobilized positive shaft resistance over a certain distance, a transition zone. The three distribution curves shown, "False", "True", and "Residual" are interdependent. That is, any two determine the third: False Distribution plus Residual Load is True Distribution. Along the upper length with fully mobilized resistance, the residual load distribution is equal to the true distribution of shaft resistance. For details, see Fellenius 2014.

In unloading the pile from the maximum load applied to the pile head, the reduction of load in the pile (as determined by the strain-gages) is larger than the increase of load for the maximum load. As the strain values at the test start is the "zero" reference for all gages, the loads measured in the gages after unloading appear to be negative as if the pile would be in tension. The reason is that the shear force building up the residual load was reduced due to the test—but not eliminated; clearly some residual load still remained in the pile.

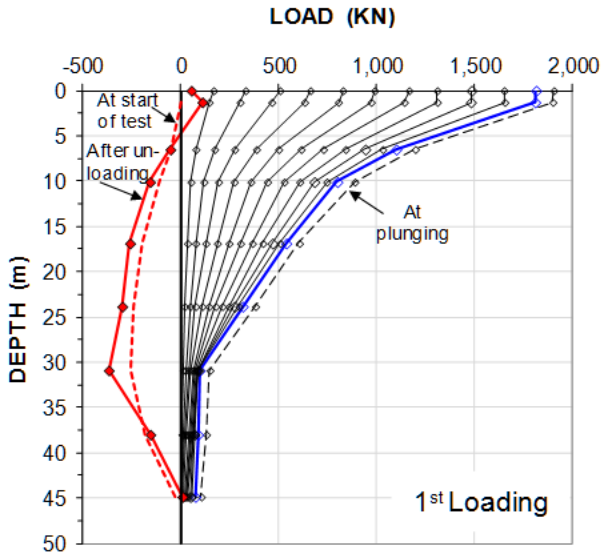

Fig. 5 Measured load distribution curves, Case 1

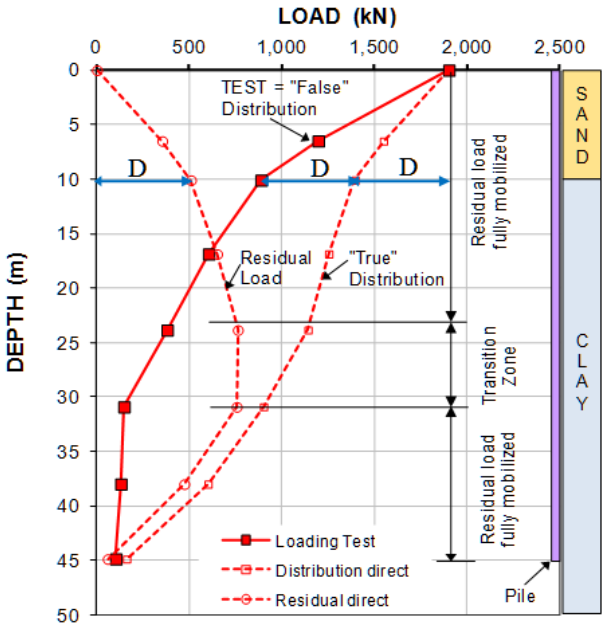

Fig. 6 "False", "True", and Residual Load Distributions, Case 1. The double-arrows labeled "D" indicate values of equal load.

The CPTU sounding records were used to calculate the pile capacity according to the LCPC and Schmertmann CPT-methods and the E-F CPTU-method (Eslami and Fellenius 1997, Fellenius 2014). The calculations were made using the software UniPile5 (Goudreault and Fellenius 2013). The LCPC and Schmertmann methods gave calculated values of 1,230 and 907 kN, respectively, while the E-F method resulted in a calculated capacity of 1,870 kN, very close to the ultimate resistance of 1,900 kN found in the static

loading test. The analysis of the CPTU records also provided the resistance distribution, supposedly, the "True" distributions. Figure 7 shows the resistance distribution calculated by the E-F method added to the distributions shown in the previous figure. The "Residual CPTU" curve is the CPTU-determined resistance (assumed as "True") minus the test values. The so determined distributions are as plausible as the distributions determined by the direct method.

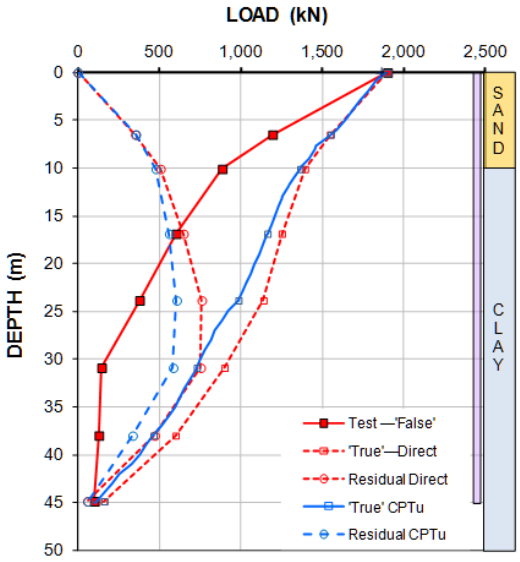

Fig. 7 Load distributions, Case 1

The CPTU-method results in a longer transfer zone as opposed to that determined directly from the strain-gage loads. However, the difference between the two methods, the direct method and the CPTU-method is otherwise slight. Both distributions correspond, approximately, to effective-stress proportionality-coefficients, beta-coefficients, of 0.6 in the sand and 0.1 in the clay, as back-calculated using UniPile5.

BORED PILE IN OOSTENDE, BELGIUM

Van Impe et al. (2013) reported the results of the static loading test on an extensometer-instrumented (tell-tales), 460-mm diameter, bored pile installed to 21.6 m depth (a full-displacement pile; Omega screw pile) through a 15 m thick old fill consisting of sand with clay deposited on about 4 m of silt and clay and 5 m of sand, followed by clay at 24 m depth. The soil profile was determined by soil sampling and a CPT-sounding (Figure 8) showing the sand to be dense between 10 to 18 m depth and very dense below 18 m depth. The piles constructed at the site were intended for support of three, 48-m diameter, 20 m high, oil-storage tanks. The assigned working load (design load) was 780 kN/pile.

Figure 9 shows the load-movement curves measured in the static loading test. The curves suggest that the pile response to the applied load was mostly from shaft resistance. What ultimate resistance to assign to the results is nebulous. The offset limit method indicates a limit load of 2,000 kN, which is usually a lower range value. An upper range value is defining the capacity as the pile head load that resulted in a 30-mm pile toe movement (marked with "+" in the figure). This indicates a capacity of about 3,100 kN made up of a toe resistance of about 400 kN and a shaft resistance of about 2,600 kN.

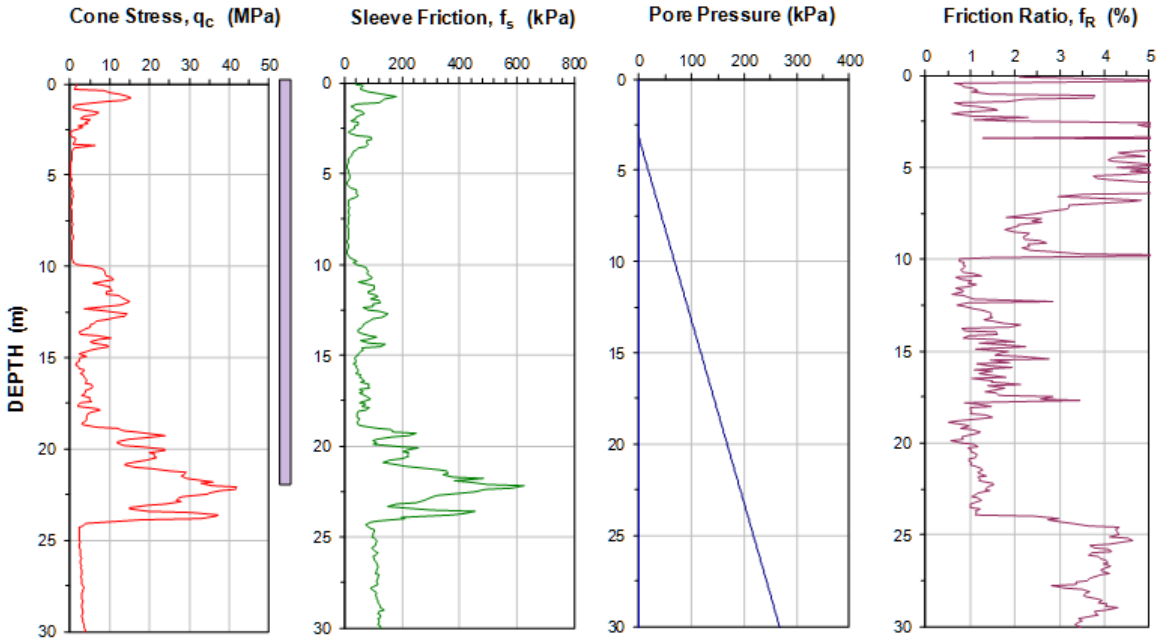

Fig. 8 CPT sounding diagram from the Oostende site, Case 2

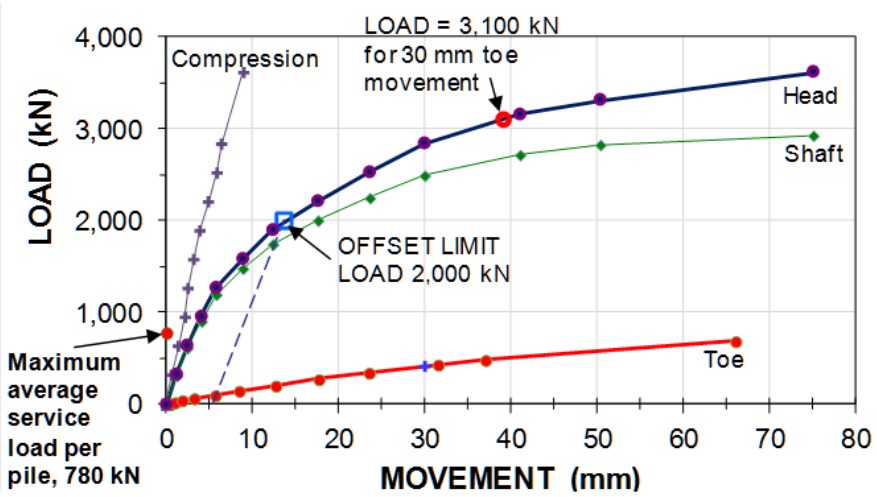

Fig. 9 Results of the static loading test: Load-movements of pile head, pile toe and shaft, Case 2

Van Impe et al. (2013) used the CPT-sounding to calculate the shaft and toe resistances of the pile. Figure 10 presents the CPT cone-stress diagram together with the CPT-calculated shaft resistance distribution and the distributions calculated using four additional methods. The figure is supplemented with the distribution of shaft resistance measured in the static loading test at the maximum applied load. The interpreted soil profile is shown to the right of the diagram. The CPT methods suggested that the ultimate shaft resistance of the test pile should be about 1,500 kN through about 2,000 kN, well below the shaft resistance implied in Figure 9.

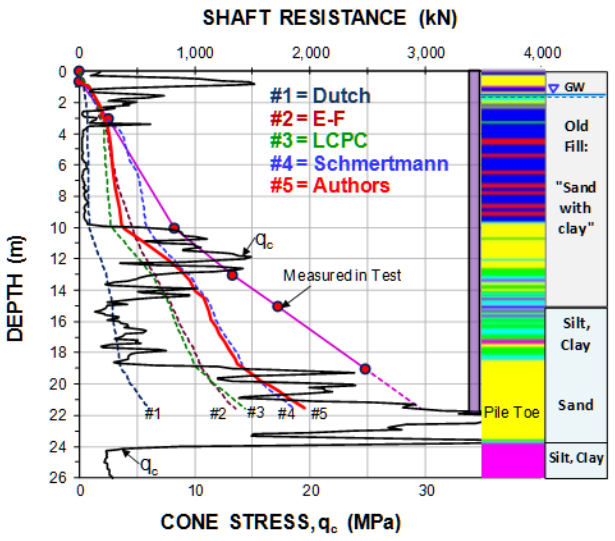

Fig. 10 Cone stress diagram and shaft resistance calculated by five CPT-methods and as measured, Case 2

Figure 11 shows the CPT-method-calculated toe resistances, suggesting that the CPT-methods have considerably overestimated the toe resistance for the test pile, as measured in the test.

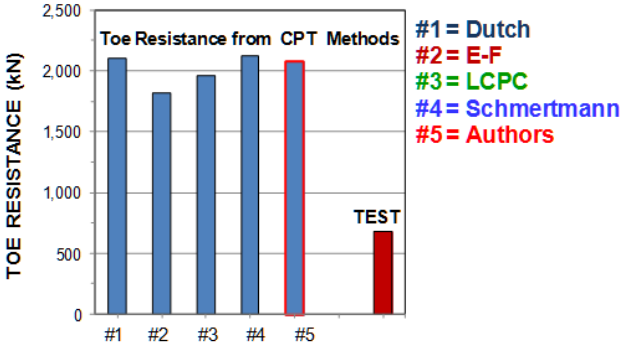

Fig. 11 Measured and CPT- and CPTU-calculated toe resistances, Case 2

Figure 12 shows the load distributions for the applied test loads. Only very little difference can be seen in the slopes of the load distributions along the pile once the applied load was larger than about 2,500 kN. The straight lines suggest that the shaft resistance can be represented in a total stress analysis by a unit shaft resistance in the upper ten meter thick backfill of 70 KPa and 150 kPa in the soil below 10 m depth, which might seem reasonable. However, when correlating the distribution to effective stress analysis, instead, a discrepancy appears: while the load distribution correlates to a beta-coefficient of 0.8 to 1.0 in the dense soil between 10 m and 18 m depth, in the very dense soil below 18 m depth, the beta-coefficient correlates to a mere 0.65. This discrepancy suggests that residual load was present in the pile before the start of the static loading test, interfering with the "Measured in Test" load distribution shown in Figure 10.

Presence of a residual load was also suggested by the authors (Van Impe et al. 2013). Figure 13 shows their "True" distribution along with the distribution determined according to the method described in the

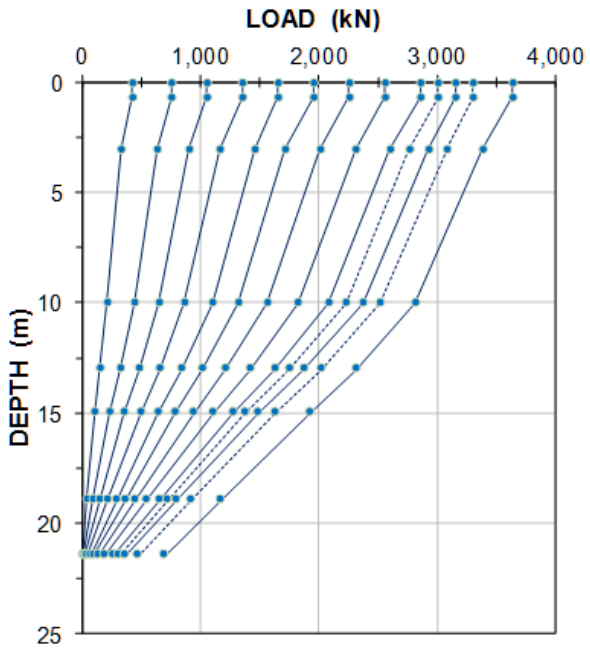

Fig. 12 Load distributions measured in the static loading test (converted from extensometer records), Case 2

foregoing. The difference between the two is that my method assumes that the residual load is due to fully mobilized negative skin friction along the entire length of the shaft, whereas I apply a transition from negative skin friction to positive shaft resistance (not fully mobilized) starting at about 17 m depth. The "True" resistance per my construction correlates to a beta-coefficient of about 0.50 in the dense sand and about 0.90 in the very dense sand, which are more plausible coefficients than those obtained when disregarding residual load.

JACK-IN SPUN-PILE IN SINGAPORE

Glostrext Technology (2013) reported results of a spun-cast cylinder pile constructed in Singapore. The soil profile consisted of sandy and gravelly silt of the Bukit Timah formation, which is a weathered in-place, granitic soil, as profiled in Figure 14. The groundwater table was close to the ground surface. The pile was a pretensioned, 600-mm diameter spun-pile with a 150-mm wall installed to 15-m embedment depth by hydraulic jacking.

The static loading test was performed two weeks after the jack-in installation of the pile to a 6,000-kN maximum installation load (probably with a small margin added). The test schedule consisted of a Cycle 1 loading of the pile from a first increment of 1,585 kN to a maximum load of 5,760 kN in seven increments, unload the pile, and, then, reload reloading the pile in a Cycle 2 applying a series of increments of same magnitude as in Cycle 1. It must be realized that Cycles 1 and 2 are really Cycles 2 and 3, because the jack-in installation of the pile constitutes a first cycle, Cycle 1. The maximum load in the reloading, Incr. #8, was 6,290 kN at which load the pile plunged when a ninth increment was being applied. Figure 15 shows the load-movement curves for the pile head, shaft, and toe, as well as the total pile shortening. The reloading curve

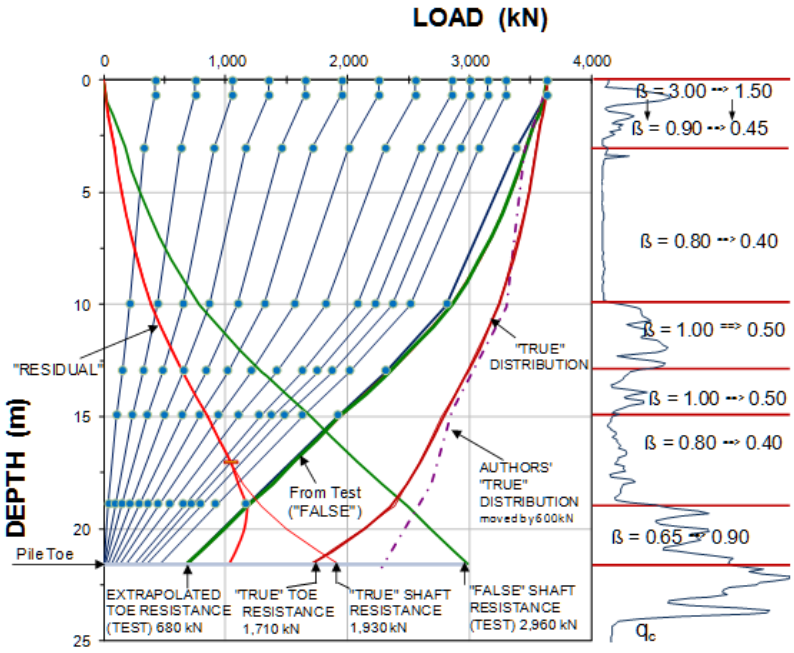

Fig. 13 Load distributions: From the test and after correction for residual load, Case 2

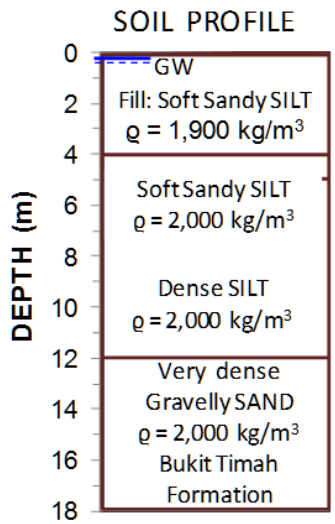

Fig. 14 Soil profile at the Singapore site, Case 3

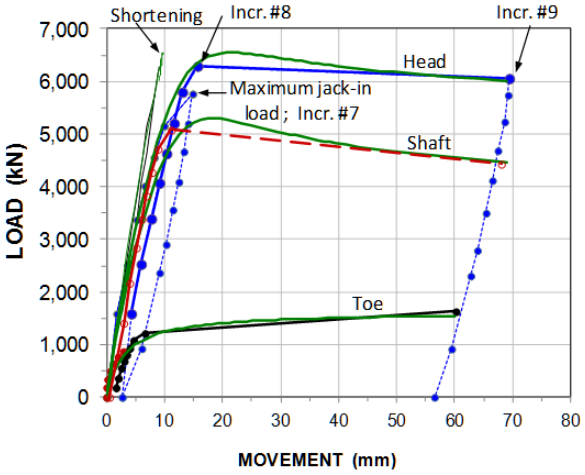

Fig. 15 Load-movement curves for pile head, toe, shaft and shortening, Case 3

(Cycle 2) is parallel to the initial load-movement curve and the unloading curves. The green lines are the load-movement curves produced in a simulation of the test, as will be explained below.

In preparation of a static loading test, two weeks after the installation, the pile was equipped with seven levels of Glostrext extensometers (Hanifah and Lee 2006), a gage system similar to a telltale system, but based on anchors and measurements of pile shortening by means of vibrating wire technology. Figures 16A and 16B show the load- distributions determined from the measured pile shortenings for both cycles of load. The distributions calculated for Increments #8 and #9 of Cycle 2 have been indicated also in Figure 16A. All loads are based on load changes from the start of Cycle 1 test (the "zero" reading).

The load distributions for Cycles 1 and 2 are remarkably similar. However, once the applied load in Cycle 2 went beyond the Cycle 1 maximum load, the Cycle 2 movement is larger. The green curve in Figure 16B is the UniPile5 fit by effective stress calculation to the measured load distribution for Cycle 2 Incr.#8. The ß-coefficients that correspond to that fit are shown in the column to the right. They are marked "False" because, above the neutral plane, they represent the sum of negative skin friction resistance and positive shaft resistance and, below the neutral plane, they exclude the positive shaft resistance already present along the pile.

The pile toe load-movement curve in Figure 15 appears to suggest that also the pile toe failed in a plunging mode after a toe penetration of about 5 mm. However, the jack-in installation method leaves the pile with a maximum residual load, including the residual load at the pile toe. Referring to Figure 2, this means that the magnitude of the residual toe load is large, leaving a rather small "false" toe resistance.

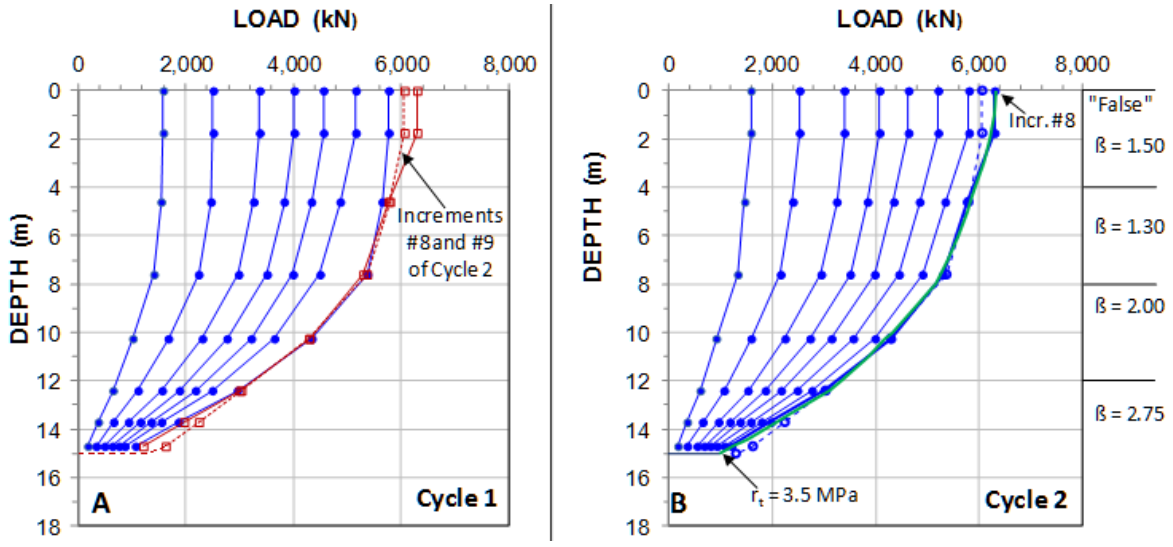

Figs. 16A and 16B Load distributions of pile head and pile toe, Cycles 1 and 2, Case 3

On the reasonable assumption that the residual load is built up from fully mobilized negative skin friction down to 12.4 m depth below which a transfer to positive shaft resistance occurs, the "True" load distribution will be as shown in Figure 17. The effective stress ß-coefficients that gave the fit to the "true" load distribution are shown in the column to the right.

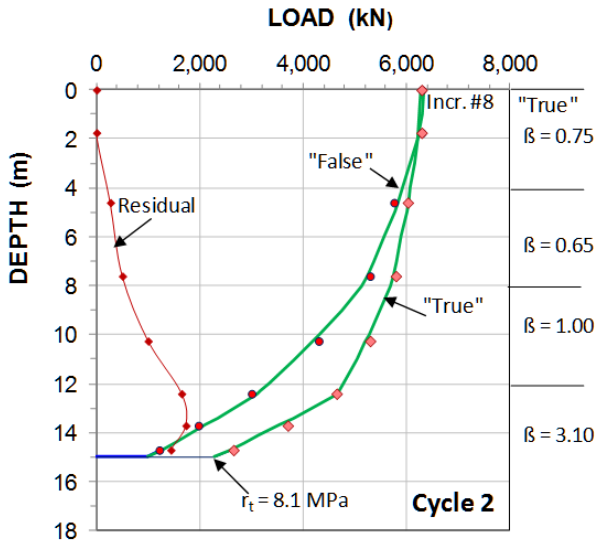

Fig. 17 "False", "True", and Residual load distributions; Cycle 2 with back-calculated beta-coefficients, Case 3

The pile bearing capacity, when based on shape of the pile head load movement curve will be larger for a pile subjected to residual load as opposed to that of a pile not affected by residual load. Figures 18A and B show a simulation of the static loading test for the test pile (18A; same as shown in Figure 15) and for a test (18B) on the identical pile that is not affected by residual load. The diagrams illustrate the difference between the two conditions. To simulate the Figure-18A diagram, effective stress coefficients shown in Figure 16B were used and the toe load-movement curve (q-z) was input as an initial reloading portion and a final portion with a flatter slope. The shaft resistance load-movement curves were input as strain-softening curve (t-z) with the peak resistance occurring at 7 mm movement and the resistance then reducing to about 80% at 70 mm movement.

Figure 18B shows that in the absence of the "preloading" provided by the residual load, the pile response the load is less stiff and the offset-limit method applied to the pile-head load-movement curve shows a significantly smaller pile capacity as does the "30-mm toe-movement" definition.

Note that the capacity determined for the jack-in pile is not "false", but true to the pile. However, the capacity determined is a function of the installation method. The load-movement curves from a test at the site on a bored pile or a driven pile with same dimension, would have shown load-movement closer to that shown in Figure 18B.

Figure 18B includes the toe load-movement of the test pile plotted at a starting point estimated to correspond to the residual load reloading condition. The curve makes reference to the notations in Figure 2.

Moreover, the difference between the two pile-toe load-movement curves is unmistakable. An ultimate toe resistance can easily be "interpreted" from the residual-load affected ("False") pile toe curve (18A). However, the pile toe load-movement curve in Figure 18B, which, in contrast, is representative for the actual pile toe response, shows no such ultimate resistance characteristic, but answers to the fact that ultimate pile toe resistance—toe capacity—is a delusion (Fellenius 1999; 2014).

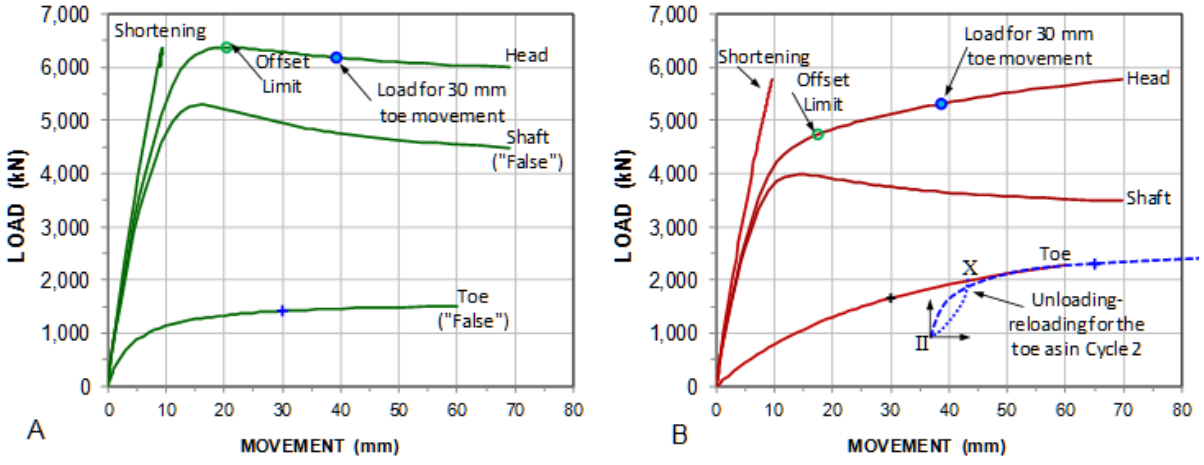

Fig. 18 Simulated static loading test results, Case 3
A. The test pile and B. A pile assumed identical but unaffected by residual load

6. CONCLUSIONS

When analyzing results from a static loading test on an instrumented test pile affected by residual load and not including the effect of the residual load, then (1) the shaft resistance along the upper portion of the pile will be overestimated, (2) the shaft resistance along the lower portion will be underestimated, and (3) the total shaft resistance will be overestimated and the pile toe resistance will be correspondingly underestimated.

The presence of residual load is not a trivial part of a pile response analysis. If it is present in a test pile, and not recognized and included in the analysis, a design relying on the analysis results could be considerably off the mark.

The presence of residual load will make for a stiffer load-movement response of a pile affected by residual load, as opposed to a case of a pile with no residual load but otherwise equal, that is, having the same true shaft and toe resistances. The total pile capacity interpreted from the load movement will then be larger than for the pile with no residual load.

The results of a test on a pile affected by residual load can easily lead—mislead—to the belief that the pile has developed an ultimate toe resistance, whereas proper consideration of the residual toe load will show that this is not the case.

References

Eslami, A. and Fellenius, B.H., 1997. Pile capacity by direct CPT and CPTU methods applied to 102 case histories. Can. Geot. Journal 34(6) 886–904.

Fellenius, B.H., 1999. Bearing capacity — A delusion? Deep Foundation Institute, Hawthorne, NJ, Proceedings of Annual Meeting, Dearborn, Michigan, October 14 16, 1999, 17 p.

Fellenius, B.H., 2002a. Determining the true distribution of load in piles. American Society of Civil Engineers, ASCE International Deep Foundation Congress, An International Perspective on Theory, Design, Construction, and Performance. Geotechnical Special Publication No. 116, Edited by M.W. O'Neill, and F.C. Townsend, Orlando, FL, Feb. 14 - 16, 2002, Vol. 2, pp. 1455–1470.

Fellenius, B. H., 2002b. Determining the resistance distribution in piles. Part 1: Notes on shift of no-load reading and residual load. Part 2: Method for Determining the Residual Load. Geotechnical News Magazine, 20 (2): 35-38, and 20 (3): 25-29.

Fellenius, B.H., 2014 . Basics of foundation design, a textbook. Revised Electronic Edition, [www.Fellenius.net], 384 p.

Fellenius, B.H., Harris, D., and Anderson, D.G., 2004. Static loading test on a 45 m long pipe pile in Sandpoint, Idaho. Can. Geot. Journal 41(4) 613-628.

Glostrext Technology, 2013. Report on results of static axial compression loading test on instrumented spun pile at Bishan Street, Singapore, Report No. S-A2-013-(2013)-CSCG-ULT1.

Goudreault, P.A. and Fellenius, B.H., 2013. UniPile Version 5, Users and Examples Manual. UniSoft Geotechnical Solutions Ltd. [www.UniSoftLtd.com]. 100 p.

Gregersen, O.S., Aas, G., and DiBiagio, E., 1973. Load tests on friction piles in loose sand. Proceedings of the 8th International Conference on Soil Mechanics and Foundation Engineering, ICSMFE, Moscow, August 12-19, 1973, Vol. 2.1, Paper 3/17, pp. 109–117.

Hanifah, A.A. and Lee S.K., 2006. Application of global strain extensometer (Glostrext) method for instrumented bored piles in Malaysia. Proc. of the DFI-EFFC 10th Int. Conference on Piling and Deep Foundations, May 31 - June 2, Amsterdam, 8 p.

Hunter A.H. and Davisson M.T., 1969. Measurements of pile load transfer. Proceedings of Symposium on Performance of Deep Foundations, San Francisco, June 1968, American Society for Testing and Materials, ASTM, Special Technical Publication, STP 444, pp. 106-117.

Nordlund, R.L., 1963. Bearing capacity of piles in cohesionless soils. ASCE Journal of Soil Mechanics and Foundation Engineering 89(SM3) 1-35.

Van Impe, P.O., Van Impe, W.F., and Seminck, L., 2013. Results of an instrumented screwpile load test and connected pile-group load-settlement behavior. Journal of Geo-Engineering Sciences, IOS Press, 1(1) 13-36.